

Dielectric dispersion behavior of $\text{Ba}(\text{Zr}_x\text{Ti}_{1-x})\text{O}_3$ solid solutions with a quasiferroelectric state

Shanming Ke,¹ Huiqing Fan,^{2,a)} Haitao Huang,^{3,a)} Helen L. W. Chan,³ and Shuhui Yu⁴

¹State Key Laboratory of Solidification Processing, School of Materials Science, Northwestern Polytechnical University, Xi'an 710072, People's Republic of China and Department of Applied Physics and Materials Research Center, The Hong Kong Polytechnic University, Hung Hom, Kowloon, Hong Kong, People's Republic of China

²State Key Laboratory of Solidification Processing, School of Materials Science, Northwestern Polytechnical University, Xi'an 710072, People's Republic of China

³Department of Applied Physics and Materials Research Center, The Hong Kong Polytechnic University, Hung Hom, Kowloon, Hong Kong, People's Republic of China

⁴Shenzhen Institute of Advanced Technology, Chinese Academy of Sciences, Shenzhen 518067, People's Republic of China

(Received 22 March 2008; accepted 4 June 2008; published online 8 August 2008)

The temperature dependence of dielectric permittivity was investigated for the barium zirconium titanate solid solution system [BZT, $\text{Ba}(\text{Zr}_x\text{Ti}_{1-x})\text{O}_3$, $0.25 \leq x \leq 0.5$]. The dielectric relaxation behavior was observed in these ferroelectrics with diffused phase transition. In contrast to the canonical relaxors such as $\text{Pb}(\text{Mg}_{1/3}\text{Nb}_{2/3})\text{O}_3$, the diffused phase transition of BZT could not be well described by the popular modified Curie–Weiss law. Quasiferroelectric state theory was introduced to explain the dielectric results of the BZT relaxors. © 2008 American Institute of Physics. [DOI: 10.1063/1.2964088]

I. INTRODUCTION

Relaxor ferroelectrics (relaxors) have been attracting much interest because of their superior physical properties, such as giant dielectric constant, extraordinary piezoelectricity, ultrahigh strain, and so on. The characteristic feature of canonical relaxors is that there is a large, diffusing, and frequency-dispersive maximum in the temperature dependence of dielectric permittivity. This broad dielectric peak is believed to originate from the polarization of nanosize regions, i.e., the polar nanoregions (PNRs) (see Refs. 1 and 2 for a review of the structure and properties of relaxors). Besides the canonical relaxors, including $\text{Pb}(\text{Mg}_{1/3}\text{Nb}_{2/3})\text{O}_3$ (PMN) (Ref. 3) and $\text{Pb}(\text{Sc}_{1/2}\text{Ta}_{1/2})\text{O}_3$,⁴ the relaxor behavior could also be observed in the systems where paraelectric phase such as $\text{Ba}(\text{Zr}_x\text{Ti}_{1-x})\text{O}_3$ (BZT) (Ref. 5) and $\text{Ba}(\text{Sn}_x\text{Ti}_{1-x})\text{O}_3$ (Ref. 6) is embedded in a ferroelectric matrix or vice versa.

$(1-x)\text{BaTiO}_3-x\text{BaZrO}_3$ (BZT) system was identified as an infinite solid solution in the 1950s.⁷ BZT exhibits a pinched phase transition at $x \sim 0.15$, that is, all the three-phase transitions corresponding to pure BaTiO_3 are merged into one broad peak.⁸ Further increases of Zr concentration would result in a ferroelectric relaxor behavior similar to that of the canonical relaxors.⁹ The ferroelectric-relaxor crossover composition of BZT has been claimed to be at $x=0.25$.⁹ Recently, BZT has shown great potential for the application in tunable microwave devices,^{10,11} due to its large dielectric nonlinearity (i.e., the dependence of permittivity on dc electric field) and low dielectric loss. However, unlike the canonical relaxors (such as PMN), an electric field does not

seem to induce a long-range polar order in BZT relaxors.¹² On the other hand, there are several evidences, which reveal that BZT might well occupy a peculiar niche in perovskite-type relaxors. The high-pressure Raman scattering investigations showed that $\text{Ba}(\text{Zr}_{0.35}\text{Ti}_{0.65})\text{O}_3$ (BZT35) behaves under high pressure similar to normal ferroelectrics, not to canonical relaxors.¹³ It has been reported that PMN shows a large heat capacity anomaly as well as a large broad dielectric peak due to the formation of PNRs.¹⁴ There is no heat capacity anomaly observed in BZT35, which implies a different relaxor state from that of PMN.¹⁵ Bokov *et al.* suggested that this should be a quasiferroelectric state by taking into account nanoscale inhomogeneities of quasiferroelectric structure in which the ferroelectric regions separated by small nonpolar Zr-rich regions.¹⁶ In this work, we present the results of dielectric studies on the solid solutions between BaTiO_3 and nonferroelectric BaZrO_3 .

II. EXPERIMENTAL PROCEDURE

The $\text{Ba}(\text{Zr}_x\text{Ti}_{1-x})\text{O}_3$ (with compositions $x=0.20-0.50$, abbreviated as BZT100x) ceramics were prepared by solid state reaction process by mixing appropriate quantities of high purity BaCO_3 , ZrO_2 , and TiO_2 raw powders. The starting materials were ball milled for 8 h in alcohol. After drying, the powders were calcined at 1200 °C for 2 h. The calcined powders were further ball milled, dried, and pressed into disks with 7% polyvinyl alcohol (PVA) addition. The pellets were sintered at 1450 °C for 16 h. For a comparative study, PMN ceramics were also fabricated by a columbite method.¹⁷

The room temperature x-ray diffraction (XRD) study was carried out on all sintered ceramics of BZT which was verified to be a single phase with the cubic perovskite struc-

^{a)}Authors to whom correspondence should be addressed. Electronic addresses: hqfan3@163.com and aphhuang@polyu.edu.hk.

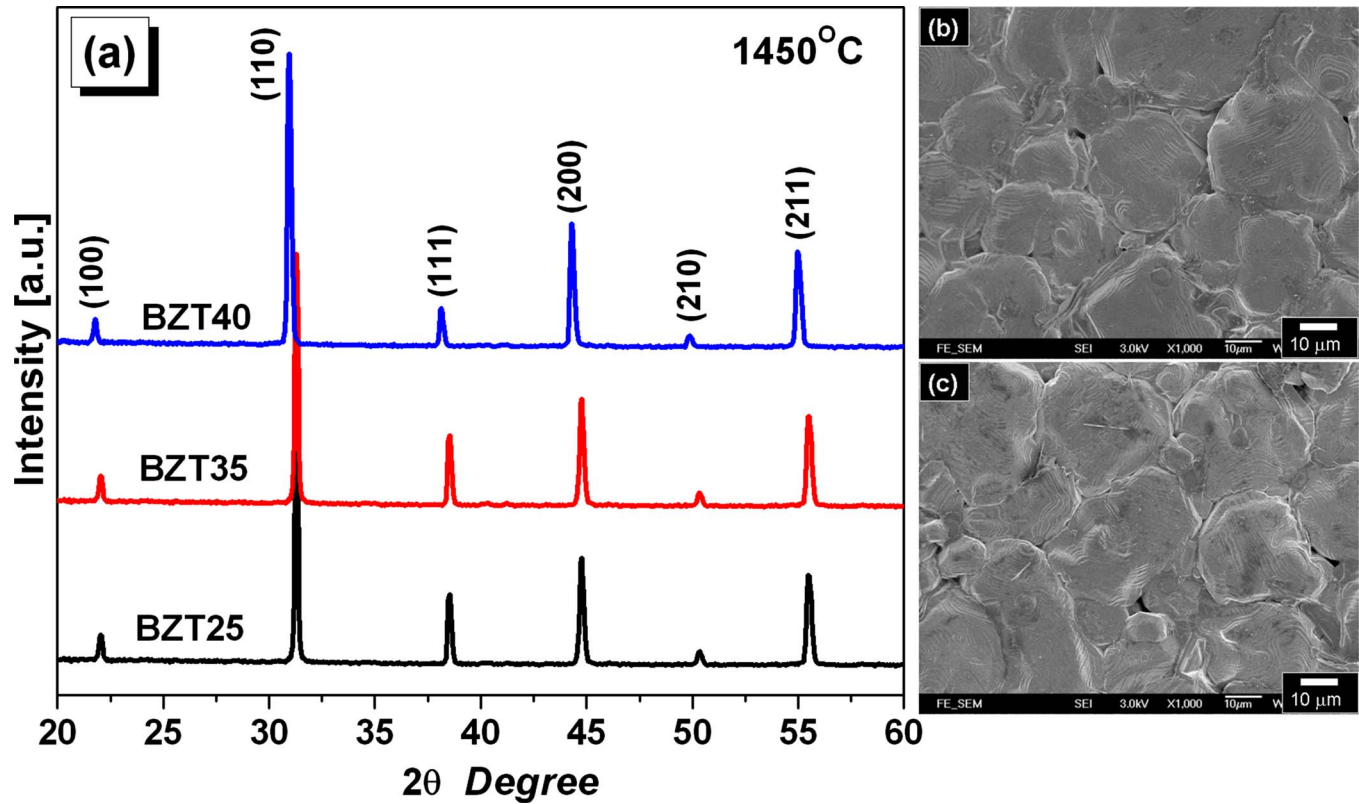


FIG. 1. (Color online) (a) XRD patterns for the BZT25, BZT35, and BZT40 ceramics sintered at 1450 °C. (b) and (c) show the FE-SEM images of the BZT25 and BZT35 surface area, respectively.

ture, as shown in Fig. 1(a). Data were collected on an automated diffractometer (X'Pert PRO MPD, Philips) with $\text{Cu } K\alpha_1$ radiation. The microstructure evolution was studied by scanning electron microscopy (SEM) (JSM-6335F, JEOL). For instance, Figs. 1(b) and 1(c) display the SEM images of BZT25 and BZT35 surfaces, respectively. The average grain size of all the ceramic samples was in the range of 10–30 μm . Micro-Raman spectral measurements were performed on a JY HR800 Raman spectrometer under back-scattering geometry. An argon ion laser was used as the excitation source with an output power of 15 mw at 488 nm. Top and bottom electrodes were made by coating silver paint on both sides of the sintered disks followed by a firing at 650 °C for 20 min. The temperature dependence of the dielectric permittivity of the samples was measured under a multifrequency LCR meter (Model SR720 of Stanford Research System), and the frequency dependence of the dielectric permittivity was measured by using a frequency response analyzer (Novocontrol Alpha-analyzer) over a broad frequency range (0.01 Hz–10M Hz).

III. RESULTS AND DISCUSSION

A. Micro-Raman scattering

The room temperature micro-Raman spectra of BZT ceramics are displayed in Fig. 2. By fitting the measured spectra and deconvolution of the fitted curves into individual Lorentzian components, the peak position of each component, i.e., the natural frequency (cm^{-1}) of each Raman active mode, was obtained in these samples. As shown in Fig. 2, the

seven normal modes of our BZT40 sample, including A1, A2, A3, A4, A5, E1, and E2 modes (where the number is only named for convenience) at 151.5, 315.9, 517.9, 723, 761.1, 230.2, and 282 cm^{-1} , respectively, are in good agreement with those of cubic $Pm3m$ BZT40 thin films.¹⁸ The dependence of the mode position on Zr concentration x is summarized in Fig. 3. In the literature, notable changes in the

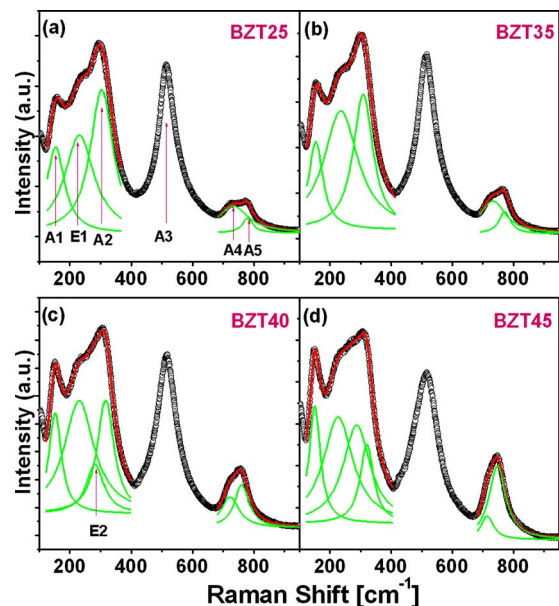


FIG. 2. (Color online) Micro-Raman scattering spectra (measured spectra: open circles and fitted spectra: thick solid lines) for (a) BZT25, (b) BZT35, (c) BZT40, and (d) BZT45 samples.

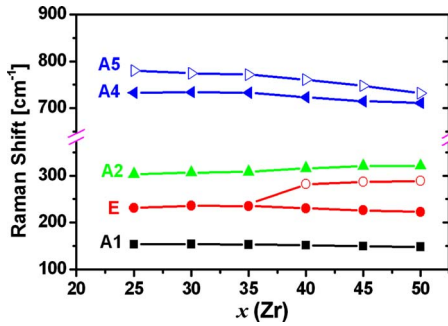


FIG. 3. (Color online) Deconvoluted active Raman mode frequencies as a function of Zr concentration x for BZT- x samples.

200–450 cm^{-1} spectral region of ferroelectric perovskites have been attributed to vibrations associated to polar BO_6 octahedra. The splitting of $E(\text{TO}_2)$ mode into $E1$ and $E2$ modes for $x \geq 0.4$ should be associated with an increase in the ionic radius [$R(\text{Ti}^{4+})=0.0745$ nm, $R(\text{Zr}^{4+})=0.086$ nm], when Ti is gradually replaced by Zr. The vibration of Ti atoms against the oxygen cage results in an $A(\text{TO}_1)$ mode at 180 cm^{-1} .¹⁹ Dobal *et al.*²⁰ reported that the $A(\text{TO}_1)$ mode could be reduced to about 129 cm^{-1} for Zr replacing Ti sites. The A1 mode frequency of our BZT samples decreases from 153.3 ($x=0.25$) to 147.88 ($x=0.50$) could therefore be assigned to a normal mode involving Zr atoms. The coupling between the A4 and A5 modes strengthens as the intensity of the A4 mode decreases with increasing Zr content. In addition, the intensity of the A5 mode at 780 cm^{-1} increase with increasing Zr content, where the mode has been claimed to be a clear signature of the relaxor phase.²¹

B. Dielectric behavior

The temperature dependence of ϵ' and the imaginary part of the dielectric constant ϵ'' at various frequencies for the BZT25, BZT35, and BZT40 samples are shown in Fig. 4. Only one broad dielectric peak is observed for all the BZT compositions. At $x=0.25$, slight frequency dispersion in ϵ' starts to appear, A stronger frequency dispersion is observed for BZT35 and BZT40. Similar to a typical ferroelectric relaxor, as the frequency increases, ϵ' decreases and the temperature (T_m) corresponding to the dielectric maxima shifts to higher values. In the same manner, the temperature of the imaginary part maxima increases with the increase of frequency, while the peak value increases unlike that of ϵ' . The decrease in T_m and the maximum dielectric constant with increasing Zr content can be well understood by phenomenological theory.²² Since Zr^{4+} has larger ionic size as compared to Ti^{4+} , the addition of Zr increases the “chemical pressure” imposed on the surrounding lattice and therefore results in lower T_m and lower maximum dielectric constant.

C. Characterization of the ϵ' peak

Since Smolensky’s work,³ the feature of the temperature dependence of the dielectric constant, above T_m , has been widely studied with various models as an important feature to characterize the dielectric relaxation behavior of a relaxor. For a normal ferroelectric, the Curie–Weiss (CW) law is fol-

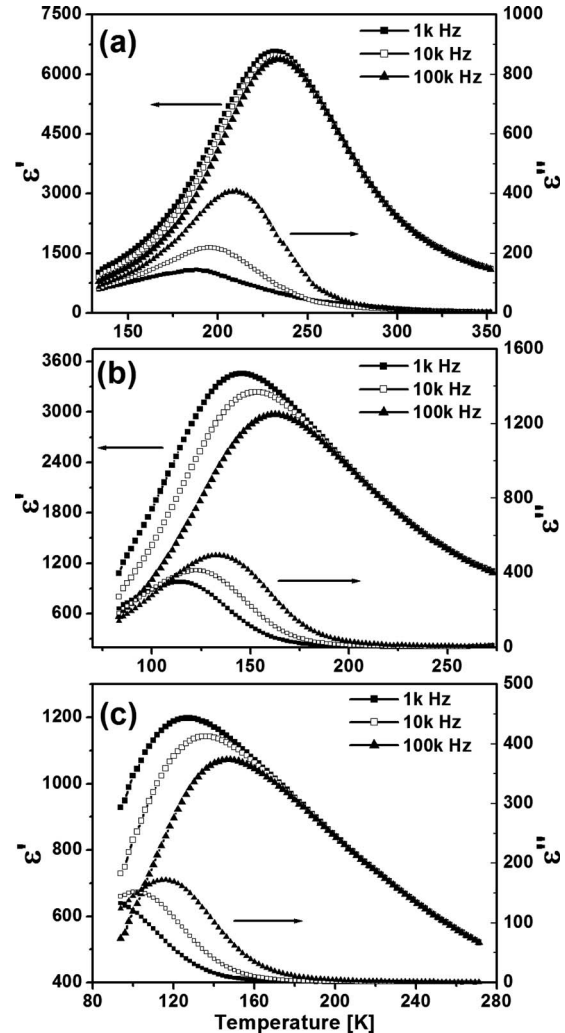


FIG. 4. Temperature dependences of the dielectric permittivity of (a) BZT25, (b) BZT35, and (c) BZT40 at various frequencies.

lowed in the paraelectric region. However, for relaxors, the dielectric constant follows CW law only above the Burns’ temperature (T_B), which is much higher than T_m and below which the PNRs appear.

A modified CW law was usually used to describe the ϵ' peak on the high temperature side and the diffuseness of the phase transition²³

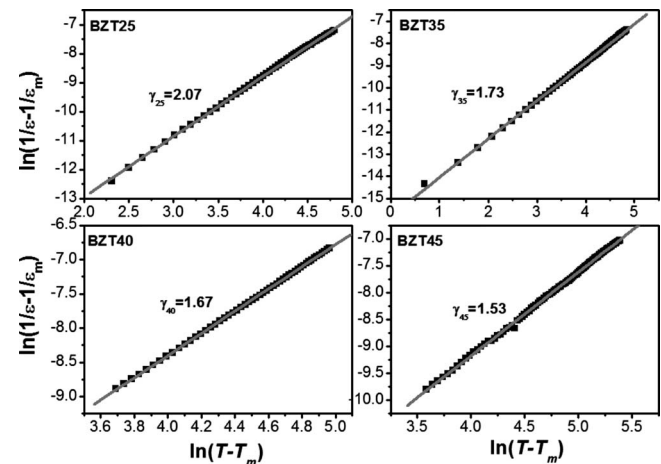


FIG. 5. Power law [Eq. (1)] fit of the reciprocal dielectric constant of BZT.

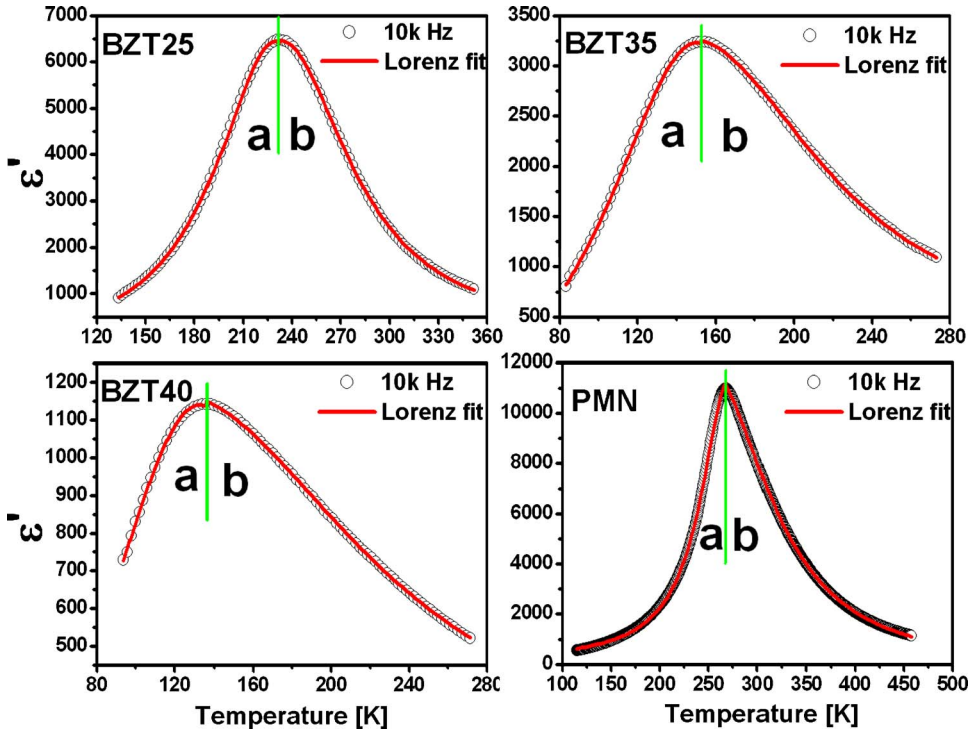


FIG. 6. (Color online) Temperature dependences of the dielectric constant of BZT25, BZT35, BZT40, and PMN at 10 kHz. The solid lines are the fitting curves by using Eq. (2).

$$1/\varepsilon - 1/\varepsilon_m = (T - T_m)^\gamma / C. \quad (1)$$

The value of γ ($1 \leq \gamma \leq 2$) is the expression of the degree of dielectric relaxation in a ferroelectric. When $\gamma=1$, Eq. (1) expresses the CW behavior of the normal ferroelectrics, while $\gamma=2$ reduces to the quadratic dependence,³ which is valid for a canonical relaxor ferroelectric experimentally. In this study, the obtained values of γ (from the experimental data at 1 kHz), fitted by Eq. (1) for BZT compositions, and the fitting curves are shown in Fig. 5. It is apparent in Fig. 5 that with the increase of Zr content there is a systematic decrease in γ . Interestingly, the γ value decreases to 1.53 with the increase in Zr concentration, which evidently shows the evolution of ferroelectric relaxations from canonical relaxor to the normal ferroelectric behavior. However, the dielectric spectra (Fig. 4) and the micro-Raman scattering results (Fig. 2) show more and more clearly a relaxor behavior from BZT25 to BZT45. This phenomenon leads to a conclusion that γ is not a good parameter to express the degree of dielectric relaxation in BZT, even in BaTiO₃-based ferroelectrics or relaxors with diffuse phase transition (DPT). Furthermore, Eq. (1) contains frequency-dependent quantities T_m and ε_m . As a result, the parameters γ and C , which define the shape of the function, also depend on frequency and thereby are not fully appropriate for describing the frequency-

independent high temperature slope of the dielectric peak. These parameters (γ and C) appear to be different sometimes in different temperature intervals for the same material.²⁴ For BZT25, γ decreases to 1.83 in a smaller temperature interval in our study.

Bokov *et al.* recently proposed a Lorentz-type formula to describe the dependence of the dielectric constant on temperature at $T > T_m$ in relaxors,²⁵

$$\frac{\varepsilon_A}{\varepsilon} = 1 + \frac{(T - T_A)^2}{2\delta^2}, \quad (2)$$

where the temperature (T_A) and the magnitude (ε_A) of the Lorentz height generally differ from the T_m and ε_m of the experiments. The parameter δ , which is frequency-independent at high enough frequencies, characterizes the diffuseness of the peak. The behavior of the dielectric constant peak on the high temperature side predicted by Eq. (2) has been found in a number of relaxor ferroelectrics,^{25,26} as well as in our prepared BZT25, BZT35, and BZT40. Excellent fits are achieved above T_m . The result of fitting is shown in Fig. 6 by solid line and the best-fit parameters are listed in Table I. Note that the increase of δ with increasing Zr concentration in BZT (from 71.7 to 170.2 in this study) indicates an increased degree of diffuseness of the dielectric peak. It

TABLE I. Curve fitting results for BZT and PMN.

Compositions	f (kHz)	T_m (K)	ε_m	T_A (K)		ε_A		δ (K)		T_L (K)
				a	b	a	b	a	b	
BZT25	10	232.5	6474.4	230	233.3	6751	6364	64	72	203
BZT35	10	152.6	3237.3	150.4	147.6	4232	3081	82.6	114.4	143
BZT40	10	136.1	1142.9	133.1	120.4	1836	1040	103.3	166.7	120
PMN	10	267.7	10986	271.1	250.6	11225	11954	48.9	103.6	264.3

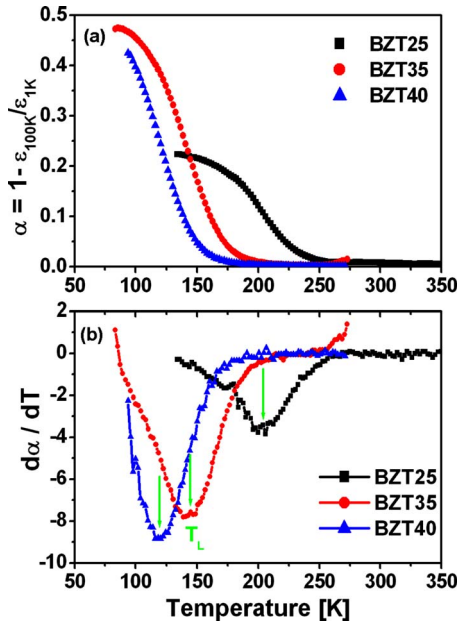


FIG. 7. (Color online) (a) The dielectric dispersion strengths ($\alpha=1-\epsilon_{100\text{KHz}}/\epsilon_{1\text{KHz}}$) for BZT25, BZT35, and BZT40 samples. (b) The $d\alpha/dT$ of BZT25, BZT35, and BZT40.

should be mentioned that Eq. (2) not only could be used to describe the high temperature side of the dielectric peak, but also the low temperature side of the dielectric peak, as shown in Fig. 6.

D. Characterization of the extent of dielectric dispersion

In Fig. 4 we note that frequency dispersion is observed for BZT ceramics, especially for BZT35 and BZT40 with higher Zr concentrations. The parameter $\alpha=1-\epsilon_{100\text{KHz}}/\epsilon_{1\text{KHz}}$ was employed to characterize the extent of the dielectric dispersion in $\text{Ba}(\text{Sn}_x\text{Ti}_{1-x})\text{O}_3$ in the previous study by the other researchers.²⁷ A bigger α implies much more dielectric dispersion. Figure 7(a) shows temperature dependency of the extent of dielectric dispersion α for BZT25, BZT35, and BZT40, respectively. The values of α for BZT35 and BZT40 show rapid decrease from about 100 to 160 K and decline to almost zero after 190 K. The values of α for BZT25 show more slowly decrease first and also decline to Zero at last. These phenomena indicate that some kinds of relaxation polarization exist in both samples of BZT35 and BZT40, which are different from BZT25. Figure 7(b) plots the differential coefficient derived from Fig. 7(a). In Fig. 7(b), we could get the characteristic temperature T_L (listed in Table I) of α , which implies the highest changing rate.

For comparison, Fig. 8 plots the temperature dependence of dielectric constant, α and $d\alpha/dT$ of PMN ceramics. It can be seen that the T_L of PMN locates at the temperature range around T_m , but T_L of BZT is 10–30 °C smaller than T_m , as presented in Table I. This phenomenon indicates that the dynamic processes of PNRs in PMN and BZT are different.

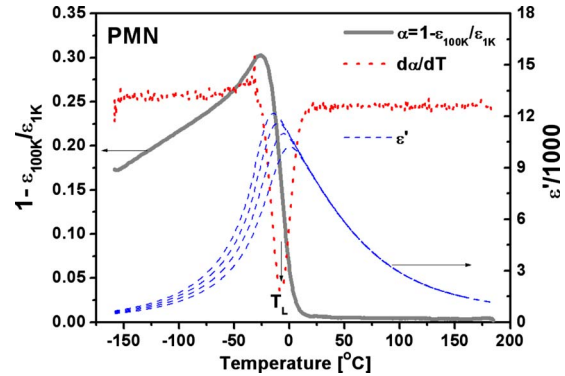


FIG. 8. (Color online) Temperature dependences of the dielectric constant (dashed line), the dielectric dispersion strength α (solid gray line), and $d\alpha/dT$ (dot line) of PMN ceramics.

E. Universal relaxor dielectric response in BZT

As shown above, in relaxor ferroelectrics (both BZT and PMN), the dielectric dispersion in the high-temperature slope of permittivity maximum ($T > T_m$) is very weak ($\alpha \rightarrow 0$) in comparison with the relaxation at $T \leq T_m$. As a result, the phenomenon was much less pronounced and had seldom been considered. Bokov and Ye²⁸ first found that at the temperatures above T_m the dielectric dispersion in $\text{Pb}(\text{Mg}_{1/3}\text{Nb}_{2/3})\text{O}_3\text{-PbTiO}_3$ (PMN-PT) exactly follows the universal dielectric response law. Figure 9 shows the frequency dependence of the real and imaginary part of the dielectric permittivity of BZT35 around and above T_m , which is similar to those reported for PMN crystal in the earlier works.^{28,29} As can be seen in Fig. 9, two processes coexist. The first one gives rise to the $\epsilon''(f)$ maximum, which is clearly seen at $T=133\text{K}$ (indicated by arrow) and the maxima move out of the measurement frequency window upon increasing temperature. The $\epsilon''(f)$ related to the second process decreases monotonically with increasing frequency (low frequency, guided by solid lines), which is more clearly shown in the ac conductivity plots ($\sigma' \sim f\epsilon_0\epsilon''$).

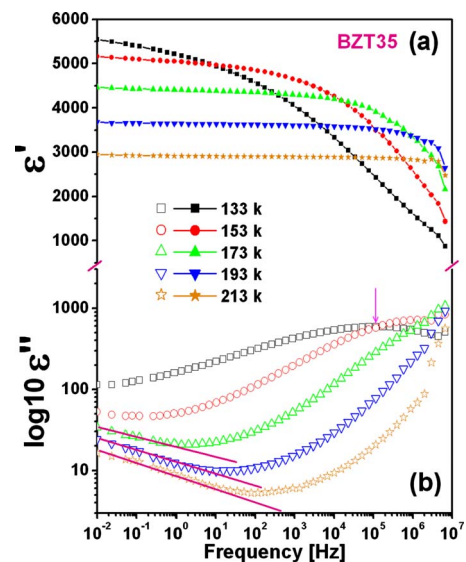


FIG. 9. (Color online) Frequency dependences of the real and imaginary part of BZT35 at temperatures around T_m . Solid line only guides the eyes.

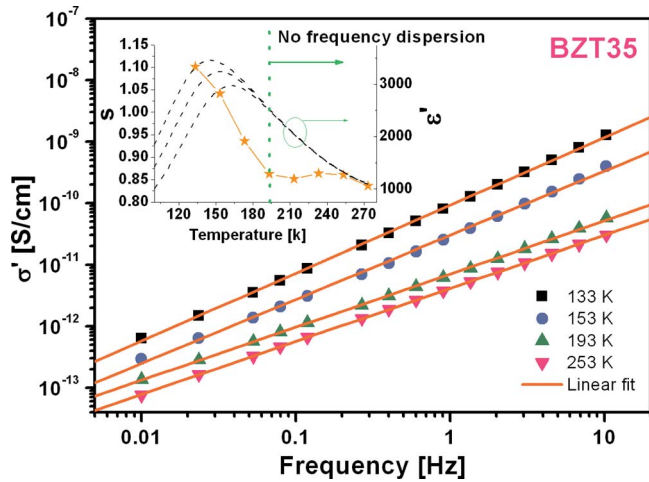


FIG. 10. (Color online) Frequency dependence of the real part of ac conductivity for BZT35. The inset shows the evolution of the exponent s [the $\epsilon'(T)$ is also shown as a reference]

Figure 10 displays the frequency dependence of the real part of ac conductivity of BZT35 at various temperatures. Obviously, it could be described by the so-called “universal dielectric response” law,

$$\sigma'(f) = \sigma_{dc} + \sigma_0 f^s, \quad (3)$$

where σ_{dc} is the dc bulk conductivity and f is the frequency. Equation (3) is typical of thermally assisted tunneling between localized states. This law describes one phenomenon that is associated with many-body interactions between charges and dipoles. By using Eq. (3), we get the exponent s as shown in the inset of Fig. 10. It can be found that s decreases rapidly with increasing temperature below 195 K, above which it gets to a plateau value. Consequently, the high-temperature dielectric dispersion of BZT tends to disappear above this temperature, which is similar to those reported by Bokov and Ye.²⁸ It is worth noting that the value of dielectric constant contributed by the universal relaxation process is much less than that of the conventional relaxor process.

F. Dielectric behavior with applied electric field

The dielectric permittivity (ϵ' and ϵ'') for BZT25, studied at various frequencies under 0 and 15 kV/cm dc biases, are shown in Fig. 11. It is evident in the figure that there is a strong response of dielectric permittivity to the applied electric field. Note that under a dc bias field of 15 kV/cm, the phase transition peak becomes much broader. Moving to higher temperatures and dielectric frequency dispersion is suppressed around the peak. However, unlike PMN and $\text{Pb}_{1-y/4}\text{La}_y(\text{Zr}_x\text{Ti}_{1-x})\text{O}_3$ (PLZT), an electric field does not seem to induce a long-range polar order.

G. Discussion

Based on the above results and analysis, it is found that BZT ($x \geq 0.25$) systems possess the basic characteristics of relaxors. The peak of $\epsilon'(T)$ is very diffusing, with a strong dispersion at the low temperature side of T_m . Our dielectric study on BZT shows a strong deviation from the CW law,

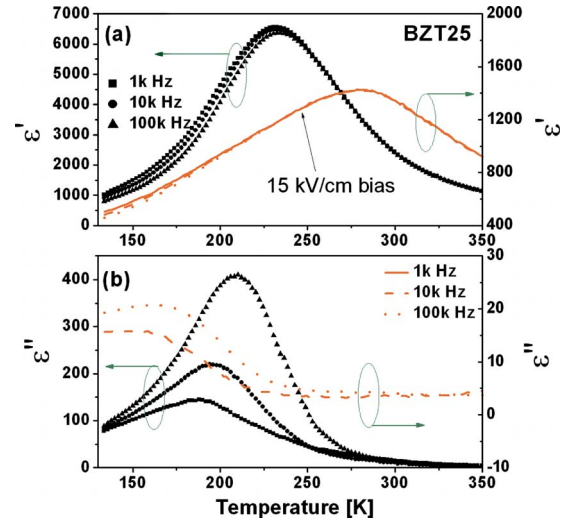


FIG. 11. (Color online) Temperature dependences of the dielectric permittivity at various frequencies for BZT25 (solid line). The dielectric permittivity under applied dc bias of 15 kV/cm is also shown (dashed line).

indicating the existence of PNRs at $T > T_m$. The XRD (Ref. 12) and Raman spectra results¹³ confirmed the absence of a structure phase transition around the T_m in BZT. Similar to PMN, the dielectric permittivity of BZT also has two main contributors: conventional relaxor dielectric response and universal relaxor dielectric response.²³ However, BZT also shows very different dielectric properties from that of the canonical relaxors. The most popular formula [Eq. (1)] is not suitable to describe the diffuseness of the DPT of BZT. The dielectric dispersion behavior of BZT is different from canonical relaxors such as PMN. Moreover, BZT relaxors display very different electric field tunable behavior compared with PMN. The reported high-pressure Raman spectra of BZT relaxors were reminiscent of features that have been observed for pure BaTiO_3 , but different from PMN.¹³

Although the step for understanding the physical phenomenon of relaxor ferroelectrics has still been going on, in canonical relaxors such as PMN, the relaxor behavior is assigned to the non-homogeneous distribution of the Mg^{2+} and Nb^{5+} cations over the B -site of the perovskite structure.¹⁻³ In contrast, for BZT, the B -sites cations have the same charge and cannot induce such a kind of charge imbalanced order-disorder. However, an inhomogeneous distribution should be at the origin of relaxor behavior. For canonical relaxor, Moriya *et al.*¹⁴ found a broad heat capacity anomaly in PMN and $\text{Pb}(\text{Mg}_{1/3}\text{Ta}_{2/3})\text{O}_3$ (PMT), which was not detected in BZT relaxors.¹⁵ The heat capacity anomaly in PMN and PMT showed order-disorder type mechanism for formation of PNRs in the crystal. In the case of BZT, the mechanism has been suggested not to be the order-disorder type, but displacive type.¹⁵ This explanation implies that there is no glassy freezing in BZT relaxors, which is in agreement with a dielectric investigation by Bokov *et al.*¹⁶ In the framework of the random bond-random field theory, freezing should lead to a decrease of entropy and then to an anomaly in the temperature dependence of heat capacity.^{14,30} Because of the special state in BZT, Bokov *et al.* proposed that the state of BZT relaxors should be called a quasiferroelectric state,

which can be considered as a mixture of the randomly distributed large (static) and small (dynamic) PNRs and the nonpolar Zr-rich nanoregions.¹⁶ The quite different properties between BZT and canonical relaxors can be then related to the change of dynamic PNR number. The changing rate of α for BZT25 show more slowly decrease compared to that of BZT35 and BZT40, which also can be attributed to the different number of static and dynamic PNRs, as the different concentration of nonpolar Zr-rich nanoregions.

IV. CONCLUSION

In summary, we have prepared the $\text{Ba}(\text{Zr}_x\text{Ti}_{1-x})\text{O}_3$ ($0.25 \leq x \leq 0.5$) ceramics by conventional solid state reaction route. Through the dielectric study of this system, we have observed an obviously different relaxor behavior in BZT system compared with the canonical relaxors. The BZT relaxors display very different dielectric dispersion behavior to that of PMN. The popular modified CW law is not suitable to describe the dielectric peak of BZT but a Lorenz-type law does. A quasiferroelectric state explanation considering static and dynamic PNRs is in agreement with the experiment results.

ACKNOWLEDGMENTS

This work has been supported by the National Nature Science Foundation of China (50672075), the RFDP (20050699011), the 111 project (B08040) of MOE, and the Aeronautic Science Foundation of China (2006ZF53068), as well as by the Research Grants Council of the Hong Kong Special Administrative Region, China (Project No. PolyU5166/05E).

¹L. E. Cross, *Ferroelectrics* **151**, 305 (1994).

²A. A. Bokov and Z.-G. Ye, *J. Mater. Sci.* **41**, 31 (2006).

- ³G. A. Smolensky, *J. Phys. Soc. Jpn.* **28**, 26 (1970).
- ⁴F. Chu, N. Setter, and A. K. Tagantsev, *J. Appl. Phys.* **74**, 5129 (1993).
- ⁵Z. Yu, A. Chen, R. Guo, and A. S. Bhalla, *J. Appl. Phys.* **92**, 2655 (2002).
- ⁶V. V. Shvartsman, W. Kleemann, J. Dec, Z. K. Xu, and S. G. Ku, *J. Appl. Phys.* **99**, 124111 (2006).
- ⁷M. McQuarrie and F. W. Behnke, *J. Am. Ceram. Soc.* **37**, 539 (1954).
- ⁸Z. Yu, A. Chen, R. Guo, and A. S. Bhalla, *J. Appl. Phys.* **92**, 1489 (2002).
- ⁹A. Simon, J. Ravez, and M. Maglione, *J. Phys.: Condens. Matter* **16**, 963 (2004).
- ¹⁰Z. Yu, A. Chen, R. Guo, and A. S. Bhalla, *Appl. Phys. Lett.* **81**, 1285 (2002).
- ¹¹J. Zhai, X. Yao, L. Zhang, and B. Shen, *Appl. Phys. Lett.* **84**, 3136 (2004).
- ¹²Ph. Sciau, G. Calvarin, and J. Ravez, *Solid State Commun.* **113**, 77 (1999).
- ¹³J. Kreisel, P. Bouvier, M. Maglione, B. Dkhil, and A. Simon, *Phys. Rev. B* **69**, 092104 (2004).
- ¹⁴Y. Moriya, H. Kawaji, T. Tojo, and T. Atake, *Phys. Rev. Lett.* **90**, 205901 (2003).
- ¹⁵M. Nagasawa, H. Kawaji, T. Tojo, and T. Atake, *Phys. Rev. B* **74**, 132101 (2006).
- ¹⁶A. A. Bokov, M. Maglione, and Z.-G. Ye, *J. Phys.: Condens. Matter* **19**, 092001 (2007).
- ¹⁷H. Q. Fan, L. T. Zhang, L. Y. Zhang, and X. Yao, *Solid State Commun.* **111**, 541 (1999).
- ¹⁸A. Dixit, S. B. Majumder, P. S. Katiyar, and A. S. Bhalla, *Thin Solid Films* **447–448**, 284 (2004).
- ¹⁹A. Chaves, R. S. Katiyar, and S. P. S. Porto, *Phys. Rev. B* **10**, 3522 (1974).
- ²⁰P. S. Dabal, A. Dixit, R. S. Katiyar, Z. Yu, R. Guo, and A. S. Bhalla, *J. Appl. Phys.* **89**, 8085 (2001).
- ²¹R. Farhi, M. E. Marssi, A. Simon, and J. Ravez, *Eur. Phys. J. B* **9**, 599 (1999).
- ²²H. Huang, C. Q. Sun, Z. Tianshu, and P. Hing, *Phys. Rev. B* **63**, 184112 (2001).
- ²³K. Uchino and S. Nomura, *Ferroelectr., Lett. Sect.* **44**, 55 (1982).
- ²⁴O. Bidault, E. Husson, and P. Gaucher, *Philos. Mag. B* **79**, 435 (1999).
- ²⁵A. A. Bokov, Y.-H. Bing, W. Chen, and Z.-G. Ye, *Phys. Rev. B* **68**, 052102 (2003).
- ²⁶A. A. Bokov and Z.-G. Ye, *Solid State Commun.* **116**, 105 (2000).
- ²⁷Xiaoyong Wei, Y. J. Feng, and X. Yao, *Appl. Phys. Lett.* **83**, 2031 (2003).
- ²⁸A. A. Bokov and Z.-G. Ye, *Phys. Rev. B* **74**, 132102 (2006).
- ²⁹A. A. Bokov and Z.-G. Ye, *J. Phys.: Condens. Matter* **12**, L541 (2000).
- ³⁰M. V. Gorev, I. N. Flerov, V. S. Bondarev, and Ph. Sciau, *J. Exp. Theor. Phys.* **96**, 531 (2003).